Chinese Journal of
POLYMER SCIENCE

RESEARCH ARTICLE

https://doi.org/10.1007/s10118-026-3724-4
Chinese J. Polym. Sci.

Rod-coil Amphiphilic Block Copolymer Assisting Emulsion Confinement Self-assembly of Hydrophobic Quantum Dot into Robust Bio-imaging Nanoprobe

Jun-Ni Xie[a,b], Xiao-Ling Xu[b], Huan-Di Qiu[d], Yuan-Yuan Li[b*], Xiao-Feng Peng[b], Yu-Fei Wang[b], Xing-Bao Yang[b], Xiao-Hong He[e], Dong-Sheng Wang[a*], and Kun Jia[b,c*]

[a] *Department of Clinical Laboratory, Sichuan Clinical Research Center for Cancer, Sichuan Cancer Hospital & Institute, Sichuan Cancer Center, Affiliated Cancer Hospital of University of Electronic Science and Technology of China, Chengdu 610041, China*
[b] *School of Materials and Energy, University of Electronic Science and Technology of China, Chengdu 610054, China*
[c] *Sichuan Province Engineering Technology Research Center of Novel CN Polymeric Materials, Chengdu 611731, China*
[d] *Institute of Life Science, eBond Pharmaceutical Technology Ltd., Chengdu 611130, China*
[e] *Sichuan Meteorological Optoelectronic Sensor Technology and Application Engineering Research Center, College of Optoelectronic Engineering (College of Weather Modification), Chengdu University of Information Technology, Chengdu 610225, China*

Electronic Supplementary Information

Abstract Self-assembly of block copolymers (BCP) with quantum dots (QDs) in a three-dimensional confined emulsion system is an effective method for preparing advanced QD/polymer composite particles with diverse morphologies and functionalities. However, the obtained particles normally exhibit sub-micrometer sizes and contain residual toxic surfactants, which hinders their potential application in fluorescent bio-imaging. In this study, we designed and synthesized a rod-coil-type amphiphilic block copolymer bearing a rigid hydrophobic poly(arylene ether nitrile) (PEN) block end-capped with a flexible hydrophilic poly(ethylene glycol) (PEG) segment for the first time. Subsequently, the synthesized amphiphilic block copolymer, abbreviated as PENG, was employed as both the macromolecular surfactant and polymeric matrix to encapsulate the green-emitting oleophilic QD *via* emulsion confinement self-assembly. This process ultimately results in the generation of surfactant-free QD@PENG nanoparticles showing robust fluorescence emission over a wide pH and salt concentration range. Meanwhile, both the fine morphology and fluorescence emission of the QD@PENG nanoparticles were well preserved even after steam sterilization at 121 °C for 2 h, which is attributed to the high-temperature resistance of the rigid PEN segment. Owing to their robust fluorescence, biocompatibility, and nanoscale size (about 100 nm), the optimized QD@PENG nanoparticles exhibited good performance in fluorescent imaging of macrophage cells. The current work proves that the emerging rod-coil amphiphilic block copolymers could serve as a promising matrix for the preparation of reliable bio-imaging probes.

Keywords Amphiphilic block copolymer; Quantum dots; Rod-coil copolymer; Emulsion confinement self-assembly; Bio-imaging probe

Citation: Xie, J. N.; Xu, X. L.; Qiu, H. D.; Li, Y. Y.; Peng, X. F.; Wang, Y. F.; Yang, X. B.; He, X. H.; Wang, D. S.; Jia, K. Rod-coil amphiphilic block copolymer assisting emulsion confinement self-assembly of hydrophobic quantum dot into robust bio-imaging nanoprobe. *Chinese J. Polym. Sci.* https://doi.org/10.1007/s10118-026-3724-4

INTRODUCTION

Owing to their unique fluorescent properties, including high quantum yields, sharp emission bands, and resistance to photobleaching,[1–5] fluorescent quantum dots (QD) have been used in diverse applications such as bio-imaging,[6–8] fluorescent labeling,[9] and metal ion detection.[10,11] Although an increasing number of hydrophilic QD with good biocompatibility have been reported, commercially available QD with strong and stable fluorescence emission are oleophilic core-shell nanocrystals that contain heavy metals such as cadmium and lead.[12] Because of their hydrophobic surface ligands, these Cd-based QDs are usually dispersed in non-polar solvents and aggregate upon exposure to polar solvents, which normally leads to fluorescence quenching.[13,14] Therefore, these commercially available QDs should be modified using appropriate protocols to enhance their aqueous dispersibility and avoid potential biotoxicity.[15] Among the diverse QD surface modification strategies, the combination of QDs with tailored macromolecules has been considered one of the most effective protocols for obtaining QD-encoded polymeric composite materials, which is mainly due to the facile modulation of interactions between the QDs

* Corresponding authors, E-mail: lyy759707792@qq.com (Y.Y.L.)
E-mail: wangdongshengnc@163.com (D.S.W.)
E-mail: jiakun@uestc.edu.cn (K.J.)
Received March 2, 2026; Accepted April 21, 2026; Published online August 19, 2026

surface ligands and surrounding macromolecular segments.[16] Meanwhile, the limited fluorescence of single quantum dots can be improved by rationally embedding multiple QDs inside the polymer matrix to form various QD@polymer microparticles with much higher fluorescence emission intensity as well as diverse morphologies.[17] Therefore, different QD@polymer fluorescent microspheres have been developed and applied in various biomedical and chemical sensing fields.[18,19]

Oleophilic QD can be integrated into a polymer matrix *via* three different methods.[8] First, the QDs gradually diffused into the polymeric microparticles *via* the facile swelling expansion of the macromolecule chains in non-polar solvents. For instance, Han *et al*. embedded red-emitting QD inside cross-linked polystyrene microspheres using the swelling method.[20] However, the composite microspheres obtained using this method still suffer from undesired QDs leakage, which deteriorates their long-term fluorescence stability. Different from the inclusion of QD into pre-synthesized polymeric microparticles, fluorescent QDs can be introduced into the emulsion polymerization of monomers, leading to the embedding of QDs into gradually growing polymer microparticles. Joumaa *et al*. obtained submicrometer fluorescent composite microspheres by embedding CdSe/ZnS QDs in a polystyrene matrix through fine emulsion polymerization.[21] However, the fluorescence of some QDs can be easily quenched because of the presence of highly active initiators or catalysts in the emulsion system. Moreover, emulsion polymerization protocols for preparing QD/polymer composites also have some disadvantages, such as time-consuming operation or limited choice of available monomers.[17] Combining the advantages of the previous two protocols, the emulsion confinement self-assembly of block copolymers with QD is an effective method for preparing QD/polymer composites. For instance, a series of coil-coil tri-/amphiphilic block copolymers, such as Pluronic F127 (consisting of poly(ethylene oxide) (PEO) and poly(propylene oxide) (PPO) blocks with a PEO-PPO-PEO structure), poly(styrene-*b*-poly(2-vinylpyridine)) (PS-*b*-P2VP), poly((ethylene oxide)-*b*-poly(γ-methacryloxypropyl trimethoxysilane)) (PEO-*b*-PγMPS), and poly(styrene-*b*-poly(*N*-isopropylacrylamide)) (PS-*b*-PNIPAm), have been developed to improve the water dispersion of hydrophobic QDs and obtain fluorescent composite microspheres through emulsion confinement self-assembly.[22–26] However, these copolymers, which possess only flexible alkyl backbones, suffer from limited thermal stability, which restricts their compatibility with autoclaving at 121 °C. Although He *et al*. successfully used rod-rod super-engineering thermoplastics with excellent heat resistance to fabricate fluorescent composite microspheres with stable fluorescence even under extreme conditions *via* the emulsion-confined self-assembly,[27,28] the necessity of adding surfactants (CTAB, SDS, PVP) to stabilize emulsion droplets introduced a critical drawback: some surfactants became firmly attached to the microsphere surface and could hardly be washed off, causing side effects for subsequent biomedical applications.[29,30] Meanwhile, composite microspheres obtained by the surfactant-assisted emulsion solvent evaporation method normally have large sizes of approximately several hundred nanometers,[31] which limits their potential application in cellular bio-imaging. In summary, preparing QD/polymer composite particles with smaller sizes *via* the non-surfactant emulsion evaporation-induced self-assembly process is still challenging at present.

To prepare clean and small QD/polymer composite particles, the oil-in-water emulsion droplet size during self-assembly should be decreased and stabilized without the use of additional small surfactants.[32,33] Amphiphilic block copolymers (BCP) have been considered the ideal matrix to prepare small and clean QD/polymer composite particles *via* emulsion confinement self-assembly for the following reasons. On the one hand, the amphiphilic BCP with suitable molecular weight and hydrophilicity can be directly employed as the macromolecular surfactant to form stable the O/W emulsion droplet, thus eliminating the concern of ionic surfactant residues in the final product. On the other hand, certain functional groups or active segments can be introduced into amphiphilic block copolymers, which enhances their intermolecular interactions with the surface ligands of QD. Thus, as organic solvents evaporate gradually, the interactions between the surface ligands of QDs and amphiphilic block copolymers would drive the effective encapsulation of a large amount of QDs inside the polymer matrix, while the hydrophilic segments of amphiphilic BCP facilitate stable dispersion in the aqueous phase, which finally leads to the generation of water-dispersible QD/polymer composite nanoparticles.

Based on the above discussion, the appropriate amphiphilic block copolymer should have both good hydrophilicity and strong interaction with the oleophilic surface ligands of QD. In this sense, poly(ethylene glycol) (PEG) is a typical flexible polymer with good hydrophilicity and biocompatibility.[34,35] In contrast, polyarylene ether nitrile (PEN) is a rigid polymer containing an aromatic backbone and pendent nitrile group in the side chain, which has been modified and used as a matrix to prepare sub-micrometer-sized QD-encoded composited beads *via* surfactant-assisted emulsion evaporation-induced self-assembly, according to our previously published work[36,37]. Therefore, a novel rod-coil-type amphiphilic block copolymer, named PENG, was synthesized through nucleophilic substitution copolymerization of fluorine-capped oligomer PEN with monohydroxylated oligomer PEG for the first time. Interestingly, we found that the synthesized PENG block copolymer could serve as both a macromolecular surfactant and a polymer matrix to encapsulate oleophilic QD *via* emulsion confinement self-assembly. After optimizing the PENG molecular weight and emulsion self-assembly parameters, small-sized QD@PENG nanoparticles (average diameter of about 100 nm) with ultra-stable fluorescence emission and low cytotoxicity were prepared. Owing to its reliable fluorescence emission as well as good biocompatibility, the optimized QD@PENG exhibited good bio-imaging performance towards macrophages in a proof-of-concept application.

EXPERIMENTAL

Materials

N-methylpyrrolidone (NMP), 2,6-difluorobenzonitrile (DFBN), and methylthiazolyltetrazole (MTT) powder (MB4698) were procured from Chengdu Aoshuo Biotechnology. *N*,*N*-dimethylformamide (DMF) and dichloromethane (DCM) were procured

from Chengdu Covidro Technology. Bisphenol A (BPA) and toluene were procured from Sichuan Xilong Science. The following reagents were procured from Chengdu Jiyuan Chemical Co. Hydrochloric acid (HCl), sodium hydroxide (NaOH), potassium carbonate (K_2CO_3), and polyethylene glycol monomethyl ether (mPEG; M_w=2000) were used. Core-shell semiconductor quantum dots (CdSe@ZnS) were acquired from WuHan JiaYuan Quantum Dots.

Synthesis of Amphiphilic Block Poly(arylene nitrile ethylene glycol) (PENG)

The block copolymer PENG with different molecular weights was synthesized by nucleophilic substitution copolymerization between a fluorine-end-capping hydrophobic PEN oligomer and a hydroxyl-terminated monomethyl ether PEG oligomer. Specifically, for the synthesis of PEN oligomer, we added 0.1 mol of BPA, 0.15 mol of K_2CO_3, 55 mL of NMP, 0.105 mol of DFBN, and 18 mL of toluene into a four-necked flask of 250 mL capacity. Subsequently, the flask was subjected to a heating process at 140 °C, accompanied by continuous stirring and refluxing for a period of 2 h. Subsequently, the temperature was raised to 180 °C with a heating rate of 10 °C/h by precisely regulating the toluene outflow (5–10 mL/h). Then, the mixture was held at 180 °C for 1 h to produce PEN oligomer. Subsequently, 0.004 mol of mPEG was dissolved in 30 mL of NMP, introduced into the previous PEN oligomer solution, and heated to 190 °C under N_2 for 2, 3 and 5 h to obtain PENG-7K, PENG-12K, and PENG-62K, respectively. The cooled polymer solution was then precipitated and incubated in ethanol for 12 h, followed by crushing and washing with fresh ethanol for three times. Finally, the purified block copolymer, PENG powder was dried at 60 °C. It should be noted that the overall polymerization reaction time can be varied to adjust the molecular weight of the resultant PENG block copolymers.

Preparation of QD@PENG Fluorescent Microspheres

Fluorescent QD@PENG nanoparticles were prepared using a surfactant-free soft confinement self-assembly protocol. Typically, PENG (5 mg) of different molecular weights was dissolved in 100 μL of DMF and mixed well with 900 μL of DCM solution containing green-emitting hydrophobic CdSe/ZnS QDs. Then, the mixtures were dispersed in 10 mL of aqueous solution without any additional surfactants and subjected to continuous magnetic stirring at 1000 r/min for 6 h in a sealed brown glass bottle. Subsequently, the mixture was brought to open air and further stirred at 500 r/min for 6 h to remove the volatile organic solvent DCM, which enabled the packing of amphiphilic PENG block copolymer with QD to form the QD@PENG colloidal in this process. Finally, the mixture was subjected to high-speed centrifugation at 10000 r/min for 5 min to remove large aggregates. It should be noted that the resultant supernatant was acquired as the final QD@PENG colloid solution, which was utilized in the following experiments and named QD@PENG-7K, QD@PENG-12K, and QD@PENG-62K according to the molecular weight of the corresponding PENG matrix.

MTT Cytotoxicity of QD@PENG Microspheres

Prior to the cytotoxicity experiment, the QD@PENG colloid solution was sterilized by UV sterilization and autoclaving for 2 h at 121 °C, respectively. Then, human embryonic kidney epithelial cells (293T cells) were seeded at a density of 8000 cells per well into 96-well plates and cultivated at a constant temperature for 4 h. QD@PENG nanoparticles with increasing concentrations were added to the 96-well flat-bottomed plates. The QDs@PENG nanoparticles were then co-incubated with 293T cells at a constant temperature for 24 and 48 h, respectively. The inhibition of cell proliferation was recorded using an enzyme marker and the absorbance at 570 nm was measured.[27] The formula for calculating the cell proliferation inhibition rate is as follows Eq. (1):

$$\text{Proliferation inhibition } (\%) = \left[1 - \left(\frac{A_{570\text{treatment}}}{A_{570\text{control}}}\right)\right] \times 100\% \quad (1)$$

where the optical absorbance at 570 nm for the treated and control cells is shown as $A_{570\text{treatment}}$ and $A_{570\text{control}}$, respectively.

Phagocytosis of QD@PENG Microspheres

As a proof-of-concept application, the cellular bioimaging capability of QD@PENG nanoparticles was evaluated using macrophages as model cells. Specifically, 1 mL of broth solution was injected intraperitoneally into the peritoneum of C57 BL/6 mice, and macrophages were collected aseptically from the mice after 3 days. Next, cells (macrophages) from mouse ascites were inoculated in six-well plates at a density per well (V_{cells}:V_{medium}=1×10^6:2). Cells were then co-incubated with the obtained QD@PENG microsphere solution at 37 °C for 6 h (dilution ratio of 1:50; the medium was composed of 10% fetal bovine serum + RPMI1640). Finally, the cells were imaged using a fluorescence microscope.

Characterization

Gel permeation chromatography (GPC) was used to measure the molecular weight of the amphiphilic PENG block, and Fourier transform infrared spectroscopy (FTIR) was used to identify the chemical structures. Transmission electron microscopy (TEM) was used to image the morphology of the QD@PENG nanoparticles, and their fluorescence emission spectra were recorded using a fluorescence spectrophotometer. A dynamic light scattering particle size analyzer (DLS, Malvem 2000) was used to characterize the size distribution of the polymer particles. We recorded the optical density of the cells using an enzyme marker (BioTek, Cytation TM 3) and used a laser scanning confocal microscope (Zeiss LSN 800) to observe the bio-imaging process.

RESULTS AND DISCUSSION

Synthesis and Characterization of Block Copolymer PENG

Co-self-assembly of amphiphilic BCP with semiconductor QD is a highly efficient method for producing fluorescent polymeric composite particles.[27] Emulsion confinement self-assembly is a specific methodology that involves the introduction of surfactants to decrease the surface tension at the oil-water (O/W) interface, which results in the formation of stable emulsion droplets in the reactor.[38–40] However, the small molecular surfactants, supposed to stabilize the emulsion reactor and be removed after self-assembly, would still stick on the surface of the final micro/nanoparticles even after intensive washing, according to our previous work.[37] Thus, the prepared particles suffer from potential cytotoxicity concerns due to the documented cellular toxicity of residual surfactants.[14,39,41] To stabilize O/W

emulsion droplets without the use of additional small molecular surfactants, we synthesized novel rod-coil-type amphiphilic block copolymers of PENG with different molecular weights for the first time. According to the chemical synthesis route shown in Scheme 1(a), PENG is composed of a rigid rod-like PEN segment and a flexible hydrophilic PEG coil segment; thus, it can serve as both a macromolecular surfactant and a robust matrix to encapsulate oleophilic QD. Specifically, when PENG and hydrophobic QD are introduced into an oil-in-water emulsion, the entanglement of the hydrophobic PEN segment and QD surface ligands would facilitate the embedding of QD into the interior hydrophobic cavity, while the flexible hydrophilic PEG segment would mitigate the outward water to stabilize the droplet. Along with the gradual evaporation of volatile organic solvent during self-assembly, the chain entanglement between PENG and QD surface ligands would be enhanced owing to the increased molecular packing. As a consequence, composite QD@PENG nanoparticles with ultra-stable fluorescence emission and free of residual toxic ionic surfactants were obtained from this soft confinement self-assembly process, as shown in Scheme 1(b). Owing to their unique advantages of small size (about 100 nm), ultra-stable green fluorescence under extreme conditions (high temperature, strong acid/alkaline, *etc.*), and biocompatibility, the obtained QD@PENG nanoparticles can be employed as a robust fluorescent labeling agent for monitoring mouse-derived macrophages, as illustrated in Scheme 1(c).

Because the molecular weight of macromolecular surfactants is important for the stability and size of emulsion droplets, [42,43] this work explored the effect of molecular weight on emulsion droplets. Three samples of PENG with different molecular weights were synthesized by varying the length of the PEN block. According to the GPC results shown in Table S1 (in the electronic supplementary information, ESI), the weight-average molecular weight of the 3 PENG samples could be modulated in the range of 7151–62049 Da by simply tuning the reaction time, as described in the experimental section. Thus, the obtained amphiphilic block copolymers were assigned according to their molecular weights as PENG-7K, PENG-12K, and PENG-62K, respectively. Moreover, ^{1}H-NMR and FTIR spectra were used to confirm the chemical structures of the synthesized PENG samples. The chemical structure and ^{1}H-NMR spectra of PENGs are shown in Fig. 1(A) and Fig. S1 (in ESI). The peaks at δ=3.34 ppm (*a*) and δ=3.50 ppm (*b*) corresponded to the proton peaks of methoxy (—OCH_3—) and methylene (—CH_2CH_2O—) in mPEG, consistent with previous reports.[44] The four chemical shift peaks at δ=7.52 ppm (*c*), δ=6.58 ppm (*d*), δ=7.13 ppm (*e*), and δ=7.33 ppm (*f*) could be attributed to the proton peaks of the benzene ring in PEN, while the peak at δ=1.67 ppm (*g*) was originated from the proton peak of the methyl group (—CH_3) in PEN. Additionally, the FITR spectra of all 3 PENG samples exhibit vibrational bands of —CH_3, —CH_2 and —CN at 2969, 2882 and 2230 cm^{-1}, respectively (Fig. 1B). The characteristic bands at 1245 and 1021 cm^{-1} can be attributed to the asymmetric vibration of the aryl ether (—Ar—O—Ar—). In addition, all three PENG samples exhibited an absorbance band at 1340 cm^{-1}, which was caused by the stretching vibration of the aliphatic ether group of C—O—C derived from the PEG segment. These results indicated that the obtained block copolymers were composed of PEN and PEG segments. Moreover, the thermal stabilities of these samples were further investigated by thermogravimetric analysis (TGA). The thermal stability of all samples was measured in the range of 80–800 °C at a heating rate of 20 °C/min. As shown in Fig. 1(C), the 5% heat loss temperatures ($T_{5\%}$) of PENG-7K, PENG-12K, and PENG-62K are 402.79, 404.72 and 405.19 °C, respectively. This result indicates that all the PENG samples with different molecular weights exhibited excellent thermal stability. In addition, the DSC curve of PENG-7K confirmed its thermal transition temperature exceeded 150 °C (Fig. S2 in ESI), well above the universal autoclaving temperature of 121 °C. This thermal stability supports the use of PENG-7K in the preparation of QD@PENG fluorescent composite microspheres for cellular bio-imaging.

Fluorescence Properties and Morphology of QD@PENG Nanoparticles

To clarify the stability and superiority of the surfactant-free

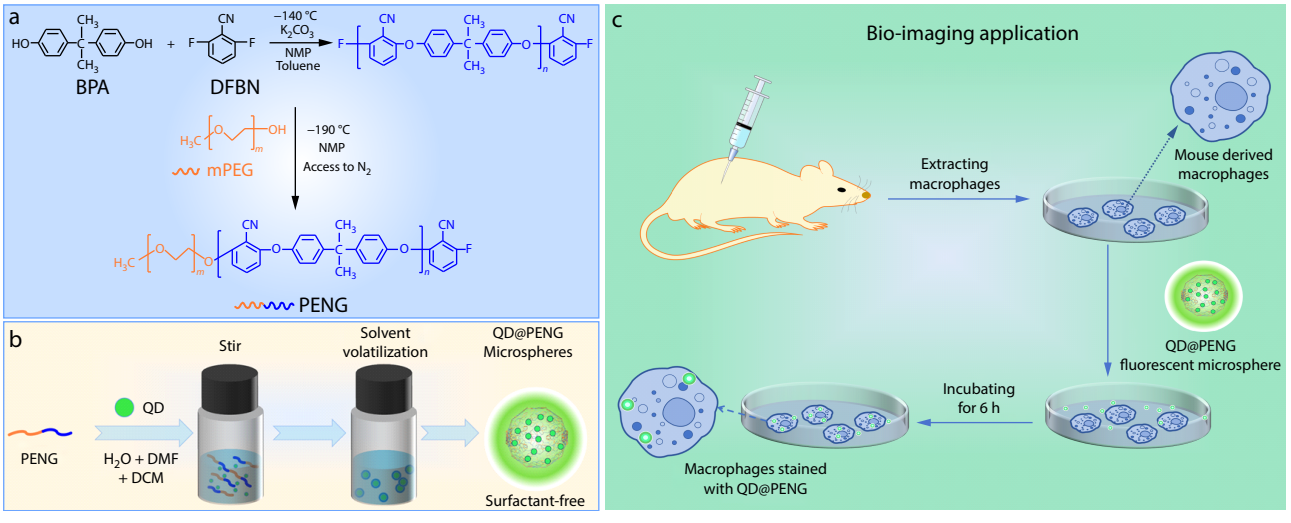

Scheme 1 (a) Chemical synthesis route of amphiphilic block copolymer of PENG; (b) Emulsion confinement co-self-assembly of hydrophobic QD with PENG; (c) Bio-imaging of mouse derived macrophages using prepared QD@PENG fluorescent nanoparticles.

https://doi.org/10.1007/s10118-026-3724-4

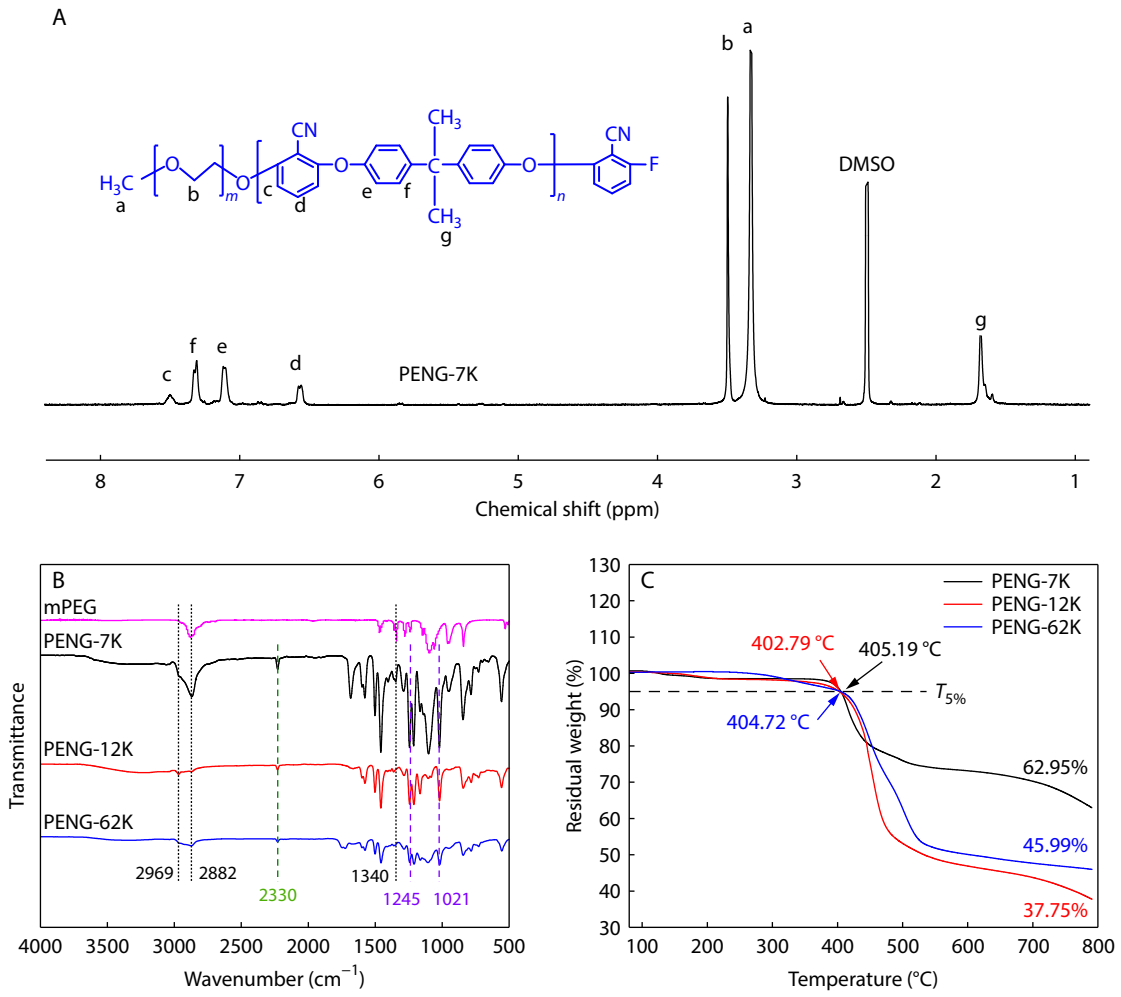

Fig. 1 Basic characterization. (A) ^{1}H-NMR spectrum of PENG-7K; (B) FTIR spectra of mPEG and the synthesized PENG block copolymers, including PENG-7K, PENG-12K, and PENG-62K; (C) TGA curves of the PENG block copolymers: PENG-7K, PENG-12K, and PENG-62K.

QD@PENG-7K fluorescent microspheres, we employed additional anionic CTAB and cationic SDS surfactants along with PENG-7K to fabricate QD@PENG-7K-CTAB and QD@PENG-7K-SDS microspheres as control groups. As shown in Figs. 2(a)–2(c), QD@PENG-7K fluorescent microspheres exhibited satisfactory fluorescence stability after dilution with surfactants (QD@PENG-7K-CTAB and QD@PENG-7K-SDS). Specifically, excellent linear relationships (R^2>99%) between the concentration and fluorescence intensity of the microspheres were observed in all three kinds of samples. As a control, QD@SDS microspheres without PENG-7K were fabricated and showed a nonlinear decrease in fluorescence intensity with increasing dilution ratio (Fig. S4 in ESI). More importantly, the QD@PENG-7K fluorescent microspheres exhibited less fluorescence intensity attenuation after being dispersed in an increasing concentration of NaCl aqueous solution, while maintaining a higher fluorescence intensity than the other two surfactant-added microspheres (Fig. 2d). These results demonstrated that the QD@PENG-7K microspheres not only possessed excellent stability comparable to that of surfactant-doped microspheres, but also displayed better salt resistance than the surfactant-doped microspheres. The desired stability and fluorescence of the QD@PENG-7K microspheres revealed the superiority of the PENG block copolymer and established a foundation for further applications in the biological field.

Subsequently, the particle size stability of the microspheres was analyzed using dynamic light scattering (DLS). As shown in Fig. S2 (in ESI) and Figs. 3(a)–3(c), the particle sizes of the QD@PENG-7K, QD@PENG-12K, and QD@PENG-62K microspheres are all concentrated at around 150 nm. The relatively small difference in the sizes of the three microspheres is possibly attributed to the rigid benzene ring structure present in the hydrophobic segments of the PENG. This structure significantly restricted the conformational flexibility of the chains. Although the hydrophobic segment of the high-molecular-weight PENG was longer, it struggled to undergo extensive coiling in an aqueous environment and instead tended to form a dense hydrophobic core through tight π-π stacking. This compact packing resulted in a hydrophobic core volume that did not increase linearly with the molecular weight, thereby reducing the size difference. After leaving the 3 types of microspheres at room temperature for one month, their particle sizes were re-evaluated to assess their long-term storage stability, as shown in Figs. 3(a)–3(c). QD@PENG-7K

https://doi.org/10.1007/s10118-026-3724-4

showed the best size stability, followed by QD@PENG-12K and QD@PENG-62K. Therefore, QD@PENG-7K and QD@PENG-12K were optimized for further studies. Given the wide pH and salt concentration range of different biological environments, the fluorescence emission of nanoparticles at different pH and salt concentrations is also important for bio-imaging application.[45] As shown in Fig. 3(d), the QD@PENG-7K and QD@PENG-12K fluorescent microspheres were tested for acid, alkali, and salt resistance. The fluorescence intensity of the QD@PENG-7K microspheres remained relatively stable over a pH range of 5–11, retaining over 50% of the fluorescence emission even at extreme pH values of 1 and 13. The QD@PENG-12K microspheres exhibited a similar trend, while their fluorescence intensity was remarkably lower than that of QD@PENG-7K. For salt resistance, the fluorescence intensity of both QD@PENG-7K and QD@PENG-12K remained relatively stable within the NaCl concentration range of 0–5 mmol/L (Fig. 3e). These findings confirm that the optimized QD@PENG microspheres exhibited good colloidal and fluorescence stability across a wide range of pH and salt concentrations.

The surface morphology of fluorescent nanoparticles is a

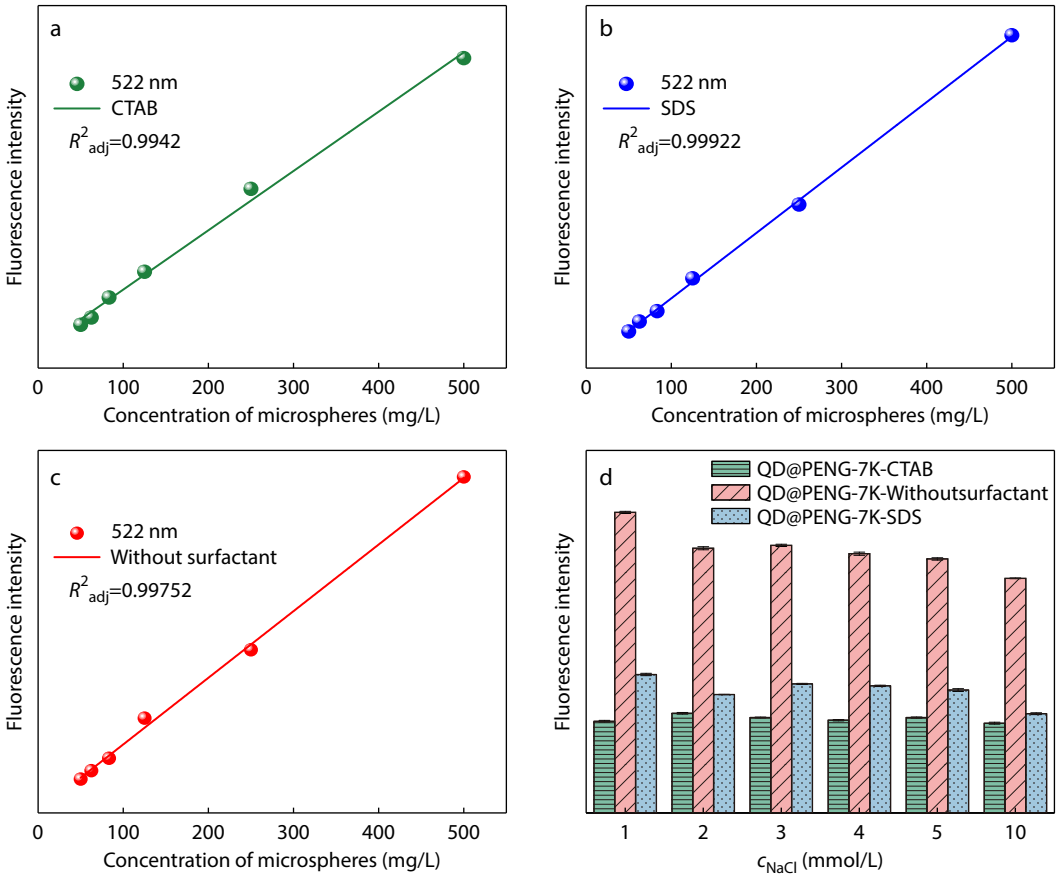

Fig. 2 Fluorescence intensity of different fluorescent microspheres. (a) Fluorescence intensity of QD@PENG-7K-CTAB microspheres; (b) Fluorescence intensity of QD@PENG-7K-SDS microspheres; (c) Fluorescence intensity of surfactant-free QD@PENG-7K microspheres; (d) Fluorescence intensity change of three kinds of microspheres with the concentration of NaCl aqueous solution.

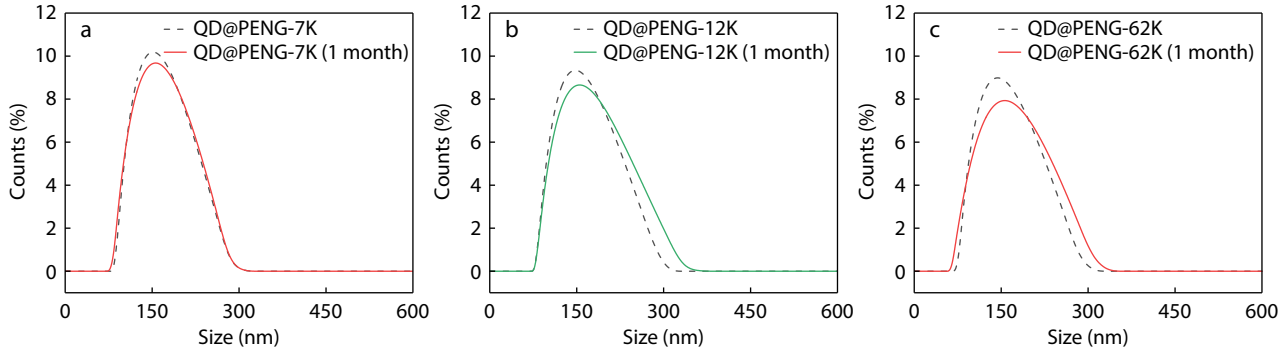

https://doi.org/10.1007/s10118-026-3724-4

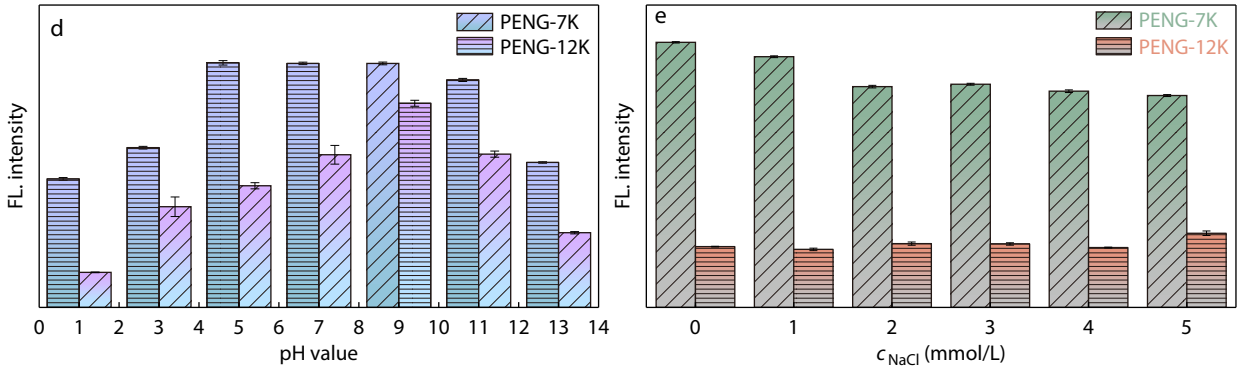

Fig. 3 Particle size distribution and fluorescence intensity of QD@PENG fluorescent microspheres. (a–c) Particle size distribution of QD@PENG fluorescent microspheres before and after one month of storage; (d) Fluorescence intensity of QD@PENG-7K and QD@PENG-12K microspheres at different pH levels; (e) Fluorescence intensity of QD@PENG-7K and QD@PENG-12K microspheres at varying salt concentrations.

pivotal aspect in determining their prospective applications. The majority of particles obtained from emulsion self-assembly of conventional BCP have a sub-micrometer size range.[46,47] However, optical cellular bioimaging normally requires much smaller fluorescent nanoparticles (about 100 nm) owing to the endocytosis process. It is fortunate that the obtained QD@PENG nanoparticles indeed exhibited smaller sizes when compared to previously reported work, as can be seen in the TEM images in Figs. 4(a)–4(c). More specifically, it is clear that the diameters of the three types of QD@PENG nanoparticles were approximately 100 nm. Among them, PENG-7K nanoparticles generally contained the highest number of encapsulated QDs, likely because of their optimal hydrophobic segment length. In contrast, the longer rigid hydrophobic segments of the high-molecular-weight PENG led to the formation of a hydrophobic core with a higher benzene-ring density and tighter packing during self-assembly. This compact structure reduced the tolerance and flexibility of the core, making it difficult for QDs to be efficiently encapsulated, thereby lowering the average QD loading per microsphere. Furthermore, the fluorescence emission spectra of the QD@PENG microspheres were recorded and presented in Fig. 4(d). The emission wavelength of QD@PENG fluorescent microspheres was located at 522 nm upon excitation with 365 nm UV light, which well matched the typical sharp emission band feature of QD. Again, the fluorescence emission intensity of QD@PENG microspheres was declined with increasing PENG molecular weight, which could be attributed to the re-

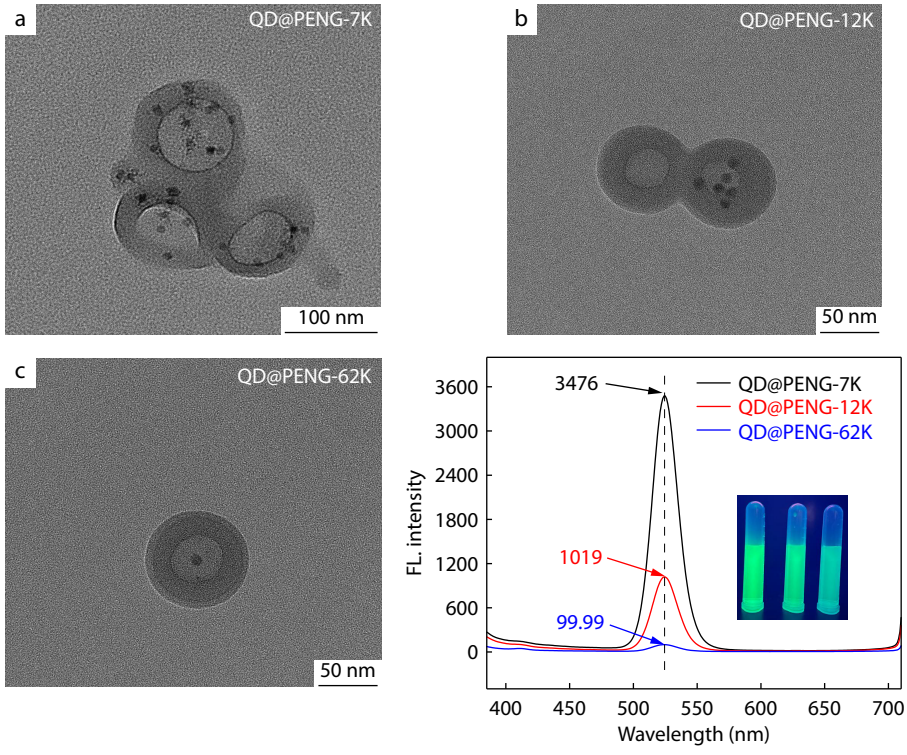

Fig. 4 TEM images of the prepared QD@PENG fluorescent nanoparticles using (a) PENG-7K, (b) PENG-12K, (c) PENG-62K, and (d) their fluorescence emission spectra.

duced QDs loading amounts. Based on these results, the QD@PENG-7K sample showed a unique size distribution, and the strongest fluorescence emission was selected as the optimal sample for subsequent experiments.

Bio-imaging Application of the Optimized QD@PENG-7K Nanoparticles

Prior to its application in cellular bio-imaging, the resistance to common sterilization and biocompatibility of fluorescent nanoparticles should be carefully evaluated.[48–50] Specifically, the fluorescence emission variation of the QD@PENG-7K nanoparticles after autoclaving (121 °C for 2 h) treatment was recorded to evaluate their resistance to sterilization, while the viability of 293T cells after incubation with increasing concentrations of autoclaved QD@PENG-7K fluorescent nanoparticles was calculated to check their biocompatibility. First, as shown in Fig. 5(a), the fluorescence emission of QD@PENG-7K nanoparticles was quite stable even after high-temperature sterilization treatment at 121 °C for 2 h. More importantly, the fine morphology of the QD@PENG-7K nanoparticles also remained almost unchanged, in accordance with the TEM images in Figs. 5(b) and 5(c). The autoclaved QD@PENG-7K colloids still showed a typical spherical morphology, accompanied by stable QDs encapsulation. This ultra-stable morphology and fluorescence emission upon sterilization could be derived from the high-temperature resistance of the rigid PEN segment, which has a high glass transition temperature of approximately 150 °C. In this sense, CdSe/ZnS QD should be firmly embedded inside the PENG matrix to avoid any possible leakage of heavy metal ions, which also ensures the excellent biocompatibility of QD@PENG nanoparticles. Indeed, according to the variation in cell viability shown in Fig. 5(d), all cell viabilities are greater than 80% after 24 h of incubation of 293T cells with different concentrations of QD@PENG-7K nanoparticles. In particular, more than 90% of the 293T cells were alive after incubation with 0.125 mg/mL QD@PENG-7K nanoparticles, which is a sufficiently high enough concentration for cellular imaging.

Based on the above results, the optimized green-emitting QD@PENG-7K nanoparticles, exhibiting stable fluorescence and good biocompatibility, were employed for further fluorescent bio-imaging. Macrophages derived from mouse enterocoelia as model cells were incubated with QD@PENG-7K fluorescent microspheres and then observed *in vitro* using fluorescence microscopy. As shown in Fig. 6, almost all macrophages were labeled by the green-luminescent QD@PENG-7K microspheres, as determined by comparing the bright-field image (Fig. 6a) with the corresponding fluorescent (Fig. 6b) and merged (Fig. 6c) images. Importantly, as illustrated in Fig. 6(d), distinct positions within an individual macrophage were illuminated by the QD@PENG-7K fluorescent microspheres. In short, owing to their biocompatibility and outstanding colloidal and fluorescence stability, our developed PENG-7K fluorescent microspheres are promising fluorophore probes for the real-time, long-term tracking of mononuclear phagocytes.

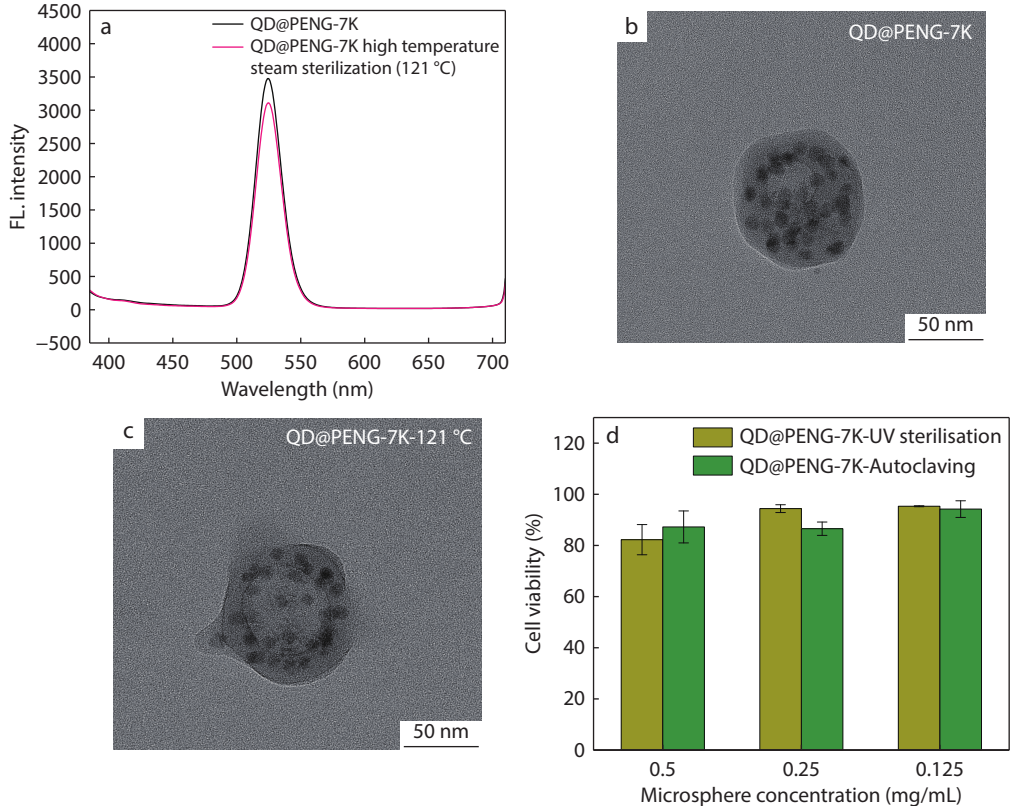

Fig. 5 Stability and cytotoxicity of autoclaved QD@PENG-7K fluorescent nanoparticles. The fluorescent emission spectra (a) and TEM images of QD@PENG-7K colloids solution before (b) and after (c) sterilization at 121 °C for 2 h. The cell viability of 293t cells (d) incubated with different concentrations of QD@PENG-7K nanoparticles for 24 h.

https://doi.org/10.1007/s10118-026-3724-4

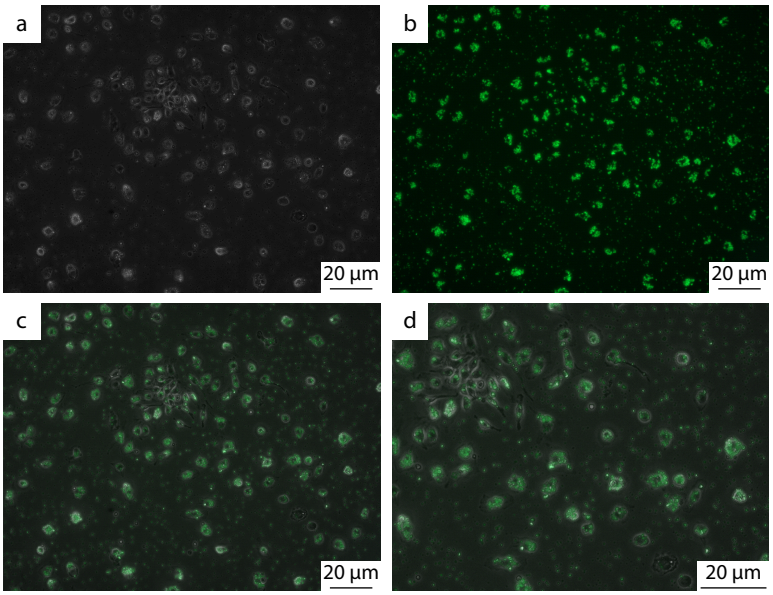

Fig. 6 The fluorescence microscope images of mouse derived macrophages stained with QD@PENG-7K fluorescent microspheres under bright field (a), fluorescent field (b), emerged fields (c) and enlarged image under emerged fields (d).

CONCLUSIONS

In this study, we successfully synthesized a novel rod-coil amphiphilic block copolymer (PENG) consisting of a rigid aromatic PEN segment and flexible hydrophilic PEG segments for the first time. Subsequently, amphiphilic PENG block copolymers were employed as macromolecular surfactants and polymeric substrates to encapsulate hydrophobic QD *via* soft confinement self-assembly. This process resulted in the generation of water-dispersible QD@PENG fluorescent nanoparticles with ultra-stable fluorescence emission and good biocompatibility. Specifically, it was found that both the size and fluorescence emission of QD@PENG nanoparticles can be modulated by changing the molecular weight of the PENG matrix. Using the PENG block copolymer with a weight-average molecular weight of 7151 Da, the obtained QD@PENG nanoparticles showed green fluorescence emission at 535 nm and an average size of approximately 100 nm. Furthermore, the spherical morphology of the nanoparticles was well preserved even after steam sterilization at 121 °C for 2 h. Moreover, the optimized QD@PENG nanoparticles also exhibited stable fluorescence when dispersed in aqueous solutions of varying pH values and exhibited good cellular biocompatibility over a wide concentration range. Owing to their appropriate diameter, good biocompatibility, and stable green fluorescence emission, the optimized QD@PENG nanoparticles exhibited good performance in the optical imaging of macrophage cells. Although biological application is still in the preliminary phase, the current work established a novel methodology for the preparation of robust, small-sized fluorescent imaging probes using rod-coil-like block copolymers.

Conflict of Interests

The authors declare no interest conflict.

Electronic Supplementary Information

Electronic supplementary information (ESI) is available free of charge in the online version of this article at http://doi.org/10.1007/s10118-026-3724-4.

ACKNOWLEDGMENTS

This work was financially supported by the National Natural Science Foundation of China (No. 22375030) and the Science and Technology Program of Sichuan Province (Nos. 2024NSFSC0263, 2024YFHZ0237 and TB2024001).

REFERENCES

1 Wang, Q.; Liu, Y.; Ke, Y.; Yan, H. Quantum dot bioconjugation during core–shell synthesis. *Angew. Chem. Int. Ed.* **2008**, *47*, 316–319.
2 He, S.; Liang, G.; Tang, B.Z.; Wu, K. Thermally activated delayed photoluminescence based on functionalized quantum dots. *Angew. Chem. Int. Ed.* **2025**, *64*, e202506555.
3 Soci, C.; Adamo, G.; Cortecchia, D.; Wang, K.; Xiao, S.; Song, Q.; Schall-Giesecke, A.L.; Cegielski, P.J.; Lemme, M.C.; Gerace, D.; Sanvitto, D.; Tian, J.; Tonkaev, P.A.; Makarov, S.V.; Kivshar, Y.S.; Jimenez Gordillo, O.A.; Melloni, A.; Pushkarev, A.P.; D'Amato, M.; Lhuillier, E.; Bramati, A. Roadmap on perovskite nanophotonics. *Opt. Mater.* **2023**, *17*, 100214.
4 Zhang, R.; Gao, S.; Cao, R. Sandwich-like QDs/MOFs films for selective sensing and multicolor emitting. *Chin. Chem. Lett.* **2022**, *33*, 4013–4016.
5 Chen, Y.; Cordero, J. M.; Wang, H.; Franke, D.; Achorn, O. B.; Freyria, F. S.; Coropceanu, I.; Wei, H.; Chen, O.; Mooney, D. J.; Bawendi, M. G. A ligand system for the flexible functionalization of quantum dots *via* Click chemistry. *Angew. Chem. Int. Ed.* **2018**, *57*, 4652–4656.
6 Ge, J.; Ma, D.; Duan, G.; Yan, Z.; Yang, L.; Yang, D.; Cai, R.; Tan, W. A novel probe for tetracyclines detection and its applications in cell imaging based on fluorescent WS2 quantum dots. *Anal. Chim.*

Graphical Abstract

Rod-coil Amphiphilic Block Copolymer Assisting Emulsion Confinement Self-assembly of Hydrophobic quantum dot into Robust Bio-imaging Nanoprobe

Jun-Ni Xie, Xiao-Ling Xu, Huan-Di Qiu, Yuan-Yuan Li, Xiao-Feng Peng, Yu-Fei Wang, Xing-Bao Yang, Xiao-Hong He, Dong-Sheng Wang, and Kun Jia

Affiliated Cancer Hospital of University of Electronic Science and Technology of China; University of Electronic Science and Technology of China; Sichuan Province Engineering Technology Research Center of Novel CN Polymeric Materials; Institute of Life Science, eBond Pharmaceutical Technology Ltd.; Chengdu University of Information Technology

A new kind of rod-coil amphiphilic block copolymer (PENG) was synthesized to use as both a macromolecular surfactant and a polymer matrix to encapsulate hydrophobic quantum dots *via* soft-confinement self-assembly, yielding surfactant-free QD@PENG water-dispersible nanoparticles with 121 °C-stable fluorescence and good biocompatibility for bio-imaging application.

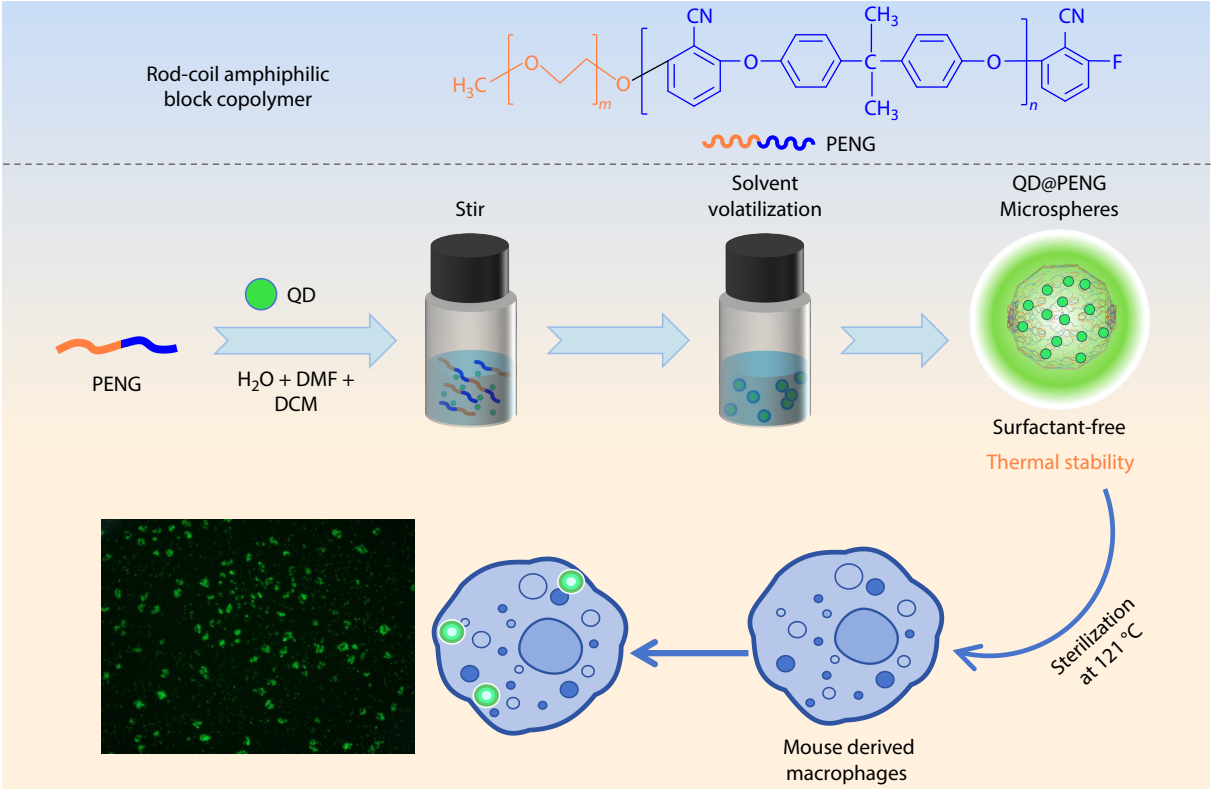

Chinese J. Polym. Sci. 2026 *https://doi.org/10.1007/s10118-026-3724-4*

Acta **2022**, *1221*, 340130.

7 Yao, F.; Wang, Z. G.; Liu, S. L.; Wang, H.; Zhu, J.; He, R.; Yang, X.; Liu, X.; Wu, Q.; Wu, J. K. Purified fluorescent nanohybrids based on quantum dot–HER2–antibody for breast tumor target imaging. *Talanta* **2023**, *260*, 124560.

8 Ma, R.; Zhou, Y.; Bi, H.; Yang, M.; Wang, J.; Liu, Q.; Huang, F. Multidimensional graphene structures and beyond: unique properties, syntheses and applications. *Prog. Mater. Sci.* **2020**, *113*, 100665.

9 Yao, Y.; Xue, J.; Wang, M.; Fu, D.; Shen, Y.; Xue, Y.; Zhang, F.; Liu, P.; Wang, H.; Wu, H. Tunable Photoluminescent, Water-Resistant and flexible films prepared using hollow Cellulose-Based microspheres encapsulating hydrophobic fluorescent dyes. *Chem. Eng. J.* **2024**, *482*, 149116.

10 Yang, Y.; Liu, X.; Meng, S.; Mao, S.; Tao, W.; Li, Z. Molecularly imprinted polymers-isolated AuNP-enhanced CdTe QD fluorescence sensor for selective and sensitive oxytetracycline detection in real water samples. *J. Hazard. Mater.* **2023**, *458*, 131941.

11 Jia, K.; Yi, K.; Zhang, W.; Yan, P.; Zhang, S.; Liu, X. Carbon nanodots

calibrated fluorescent probe of QD@amphiphilic polyurethane for ratiometric detection of Hg (II). *Sens. Actuat. B Chem.* **2022**, *370*, 132443.
12 Yang, K.; Luo, G.; Zeng, X.; Xu, M.; Pi, P.; Xu, S.; Wen, X. Aqueous quantum dots with high fluorescence, colloidal stability and biocompatibility encapsulated by an amphiphilic fluorine copolymer. *Polymer* **2019**, *179*, 121706.
13 Nie, X. B.; Yu, C. Y.; Wei, H. Precise modulation of spatially distributed inorganic nanoparticles in block copolymers-based self-assemblies with diverse morphologies. *Mater. Today Chem.* **2021**, *22*, 100616.
14 Ansari, A. A.; Lv, R.; Gai, S.; Parchur, A. K.; Solanki, P. R.; Archana; Ansari, Z. A.; Dhayal, M.; Yang, P.; Nazeeruddin, M. K.; Tavakoli, M. M. ZnO nanostructures – Future frontiers in photocatalysis, solar cells, sensing, supercapacitor, fingerprint technologies, toxicity, and clinical diagnostics. *Coord. Chem. Rev.* **2024**, *515*, 215942.
15 Farzin, M.A.; Abdoos, H. A critical review on quantum dots: From synthesis toward applications in electrochemical biosensors for determination of disease-related biomolecules. *Talanta* **2021**, *224*, 121828.
16 Chen, C.; Ng, D.Y.W.; Weil, T. Polymer bioconjugates: Modern design concepts toward precision hybrid materials. *Prog. Polym. Sci.* **2020**, *105*, 101241.
17 Khodadadi Yazdi, M.; Zarrintaj, P.; Saeb, M.R.; Mozafari, M.; Bencherif, S.A. Progress in ATRP-derived materials for biomedical applications. *Prog. Mater. Sci.* **2024**, *143*, 101248.
18 Sobiech, M.; Luliński, P.; Wieczorek, P. P.; Marć, M. Quantum and carbon dots conjugated molecularly imprinted polymers as advanced nanomaterials for selective recognition of analytes in environmental, food and biomedical applications. *TrAC, Trends Anal. Chem.* **2021**, *142*, 116306.
19 Hamed, E. M.; Li, S. F. Y. Molecularly imprinted polymers-based sensors for bisphenol-A: recent developments and applications in environmental, food and biomedical analysis. *Trends Environ. Anal. Chem.* **2022**, *35*, e00167.
20 Han, M.; Gao, X.; Su, J.Z.; Nie, S. Quantum-dot-tagged microbeads for multiplexed optical coding of biomolecules. *Nat. Biotechnol.* **2001**, *19*, 631–635.
21 Joumaa, N.; Lansalot, M.; Théretz, A.; Elaissari, A.; Sukhanova, A.; Artemyev, M.; Nabiev, I.; Cohen, J. H. M. Synthesis of quantum dot-tagged submicrometer polystyrene particles by miniemulsion polymerization. *Langmuir* **2006**, *22*, 1810–1816.
22 Yuan, Q.; Russell, T.P.; Wang, D. Self-assembly behavior of PS-*b*-P2VP block copolymers and carbon quantum dots at water/oil interfaces. *Macromolecules* **2020**, *53*, 10981–10987.
23 Lü, J.; Liu, B.; Shi, B.; Lü, C. Coordination-induced assemblies of quantum dots in amphiphilic thermo-responsive block copolymer micelles: morphologies, optical properties and applications. *Polym. Chem.* **2018**, *9*, 3158–3168.
24 Chen, H.; Yeh, J.; Wang, L.; Khurshid, H.; Peng, N.; Wang, A.Y.; Mao, H. Preparation and control of the formation of single core and clustered nanoparticles for biomedical applications using a versatile amphiphilic diblock copolymer. *Nano Res.* **2010**, *3*, 852–862.
25 Arranja, A.; Schroder, A.P.; Schmutz, M.; Waton, G.; Schosseler, F.; Mendes, E. Cytotoxicity and internalization of Pluronic micelles stabilized by core cross-linking. *J. Control. Rel.* **2014**, *196*, 87–95.
26 Bai, Q. q.; Jin, X. z.; Yang, J. h.; Qi, X. d.; Wang, Y. Constructing network structure of graphene nanoplatelets/carbon nanofibers in polystyrene and the resultant heat resistance, thermal and conductive properties. *Compos. Part A-Appl. S.* **2019**, *117*, 299–307.
27 He, X.; Ji, Y.; Xie, J.; Hu, W.; Jia, K.; Liu, X. Emulsion solvent evaporation induced self-assembly of polyarylene ether nitrile block copolymers into functional metal coordination polymeric microspheres. *Polymer* **2020**, *186*, 122024.
28 Jia, K.; Bai, Y.; Wang, L.; Luo, Y.; Hu, W.; He, X.; Wang, P.; Marks, R.; Liu, X. Emulsion confinement self-assembly regulated lanthanide coordinating polymeric microparticles for multicolor fluorescent nanofibers. *Polymer* **2021**, *230*, 124043.
29 Liang, W.; Zhao, X.; Wang, X.; Tang, Z.; Zhang, X.; Wang, X. Prediction of freshwater ecotoxicological hazardous concentrations of major surfactants using the QSAR–ICE–SSD method. *Environ. Int.* **2024**, *185*, 108472.
30 Bai, Y.; Zhang, T.; Lin, H.; Liu, X.; Guo, D.; Li, S.; Yan, D. Molecular simulation of the effect of anionic surfactant on methane diffusion in coal. *Energy* **2024**, *295*, 131018.
31 Wang, S.; Luo, L.; Wu, A.; Wang, D.; Wang, L.; Jiao, Y.; Tian, C. Recent advances in tailoring zeolitic imidazolate frameworks (ZIFs) and their derived materials based on hard template strategy for multifunctional applications. *Coord. Chem. Rev.* **2024**, *498*, 215464.
32 Soni, K. S.; Desale, S. S.; Bronich, T. K. Nanogels: an overview of properties, biomedical applications and obstacles to clinical translation. *J. Controlled Rel.* **2016**, *240*, 109–126.
33 Grason, G. M. The packing of soft materials: molecular asymmetry, geometric frustration and optimal lattices in block copolymer melts. *Phys. Rep.* **2006**, *433*, 1–64.
34 Sharma, M.; Beniwal, P.; Toor, A. P. The effect of rice straw derived microfibrillated cellulose as a reinforcing agent in starch/polyvinyl alcohol/polyethylene glycol biocompatible films. *Mater. Chem. Phys.* **2022**, *291*, 126652.
35 Gong, L.; Zhu, J.; Yang, Y.; Qiao, S.; Ma, L.; Wang, H.; Zhang, Y. Effect of polyethylene glycol on polysaccharides: From molecular modification, composite matrixes, synergetic properties to embeddable application in food fields. *Carbohydr. Polym.* **2024**, *327*, 121647.
36 Xie, J.; Jia, K.; Liu, C.; Ji, Y.; Dai, J.; Marks, R.; Liu, X. Aromatic block copolymer ligand sensitized lanthanide nanostructures as ratiometric fluorescence probe for determination of residual K_2CO_3 in super engineering thermoplastics. *Sens. Actuat. B Chem.* **2021**, *334*, 129611.
37 He, X.; Jia, K.; Marks, R.; Hu, Y.; Liu, X. 3D confined self-assembling of QD within super-engineering block copolymers as biocompatible superparticles enabling stimulus responsive solid state fluorescence. *Nano Res*. **2021**, *14*, 285–294.
38 Rayees, R.; Gani, A.; Noor, N.; Ayoub, A.; Ashraf, Z. U. General approaches to biopolymer-based Pickering emulsions. *Int. J. Biol. Macromol.* **2024**, *267*, 131430.
39 Li, Y.; Xiao, G.; Chen, C.; Chen, C.; Li, F.; Lin, L. Foam stability properties of eco-friendly three-phase foam system reinforced by polydopamine@KH560/(octyl)-trimethoxysilane modified basalt. *Colloid Surf. A-Physicochem. Eng. Asp.* **2021**, *627*, 127147.
40 Basu, M.; Hassan, P.A.; Shelar, S.B. Modulation of surfactant self-assembly in deep eutectic solvents and its relevance to drug delivery-a review. *J. Mol. Liq.* **2023**, *375*, 121301.
41 Kharaziha, M.; Scheibel, T.; Salehi, S. Multifunctional naturally derived bioadhesives: from strategic molecular design toward advanced biomedical applications. *Prog. Polym. Sci.* **2024**, *150*, 101792.
42 Singh, I. R.; Pulikkal, A. K. Nano emulsions stabilized by natural emulsifiers: A comprehensive review on feasibility, stability and bio-applicability. *J. Drug Deliv. Sci. Technol.* **2024**, *92*, 105303.
43 Durand, A.; Marie, E. Macromolecular surfactants for miniemulsion polymerization. *Adv. Colloid Interface Sci.* **2009**, *150*, 90–105.
44 Bao, D.; Liu, L.; Sun, T.; Han, Y.; Meng, F.; Zhao, M.; Yu, Y.; Guo, J.; Zhang, S. Solid solid phase change (SSPC) chitosan-*g*-mPEG fiber with improved mechanical performance *via in-situ* wet spinning process. *Carbohydr. Polym.* **2020**, *240*, 116313.

45 Lee, D. N.; Yang, S. B.; Kweon, S.; Lee, J. H.; Lee, K. J.; Ryu, Y.; Shin, D.W.; Kim, Y.J.; Lee, Y. K.; Park, J. Design and development of novel self-assembled catechol-modified bile acid conjugates as pH-responsive apical sodium-dependent bile acid transporter targeting nanoparticles. *Biomaterials* **2024**, *308*, 122539.
46 Hu, Y.; Tian, Z.; Ma, D.; Qi, C.; Yang, D.; Huang, S. Smart colloidal photonic crystal sensors. *Adv. Colloid Interface Sci.* **2024**, *324*, 103089.
47 Ganda, S.; Stenzel, M. H. Concepts, fabrication methods and applications of living crystallization-driven self-assembly of block copolymers. *Prog. Polym. Sci.* **2020**, *101*, 101195.
48 Tiwari, P.; Yadav, K.; Shukla, R. P.; Gautam, S.; Marwaha, D.; Sharma, M.; Mishra, P.R. Surface modification strategies in translocating nano-vesicles across different barriers and the role of bio-vesicles in improving anticancer therapy. *J. Controlled Rel.* **2023**, *363*, 290–348.
49 Kumar, A. M.; Khan, A.; Hussein, M. A.; Khan, M. Y.; Dafalla, H.; Suresh, B.; Ramakrishna, S. Hybrid nanocomposite coatings from PEDOT and BN-TiO_2 nanosheets: enhanced *in vitro* corrosion resistance, wettability and biocompatibility for biomedical applications. *Prog. Org. Coat.* **2022**, *170*, 106946.
50 Mohammadi, M.; Ahmed Qadir, S.; Mahmood Faraj, A.; Hamid Shareef, O.; Mahmoodi, H.; Mahmoudi, F.; Moradi, S. Navigating the future: microfluidics charting new routes in drug delivery. *Int. J. Pharm*. **2024**, 124142.

https://doi.org/10.1007/s10118-026-3724-4